# Journal of Materials Chemistry A

Accepted Manuscript


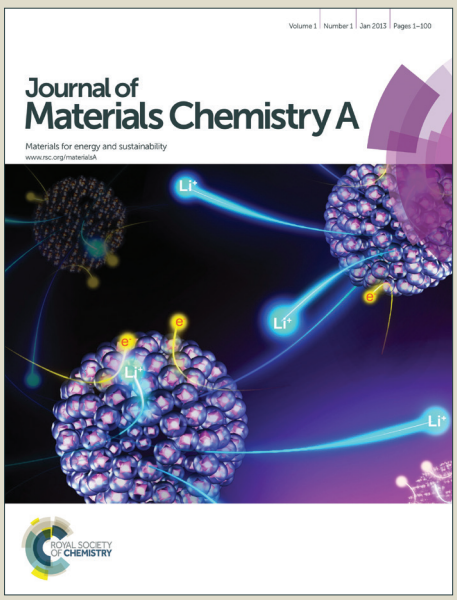





ROYAL SOCIETY OF CHEMISTRY

www.rsc.org/materialsA

Journal of Materials Chemistry A

Dynamic Article Links ►

Cite this: DOI: 10.1039/c0xx00000x

FULL PAPER

www.rsc.org/xxxxxx

# Polymer Casting of Ultralight Graphene Aerogels for the Production of Conductive Nanocomposites with Low Filling Content

**Han Hu,[a] Zongbin Zhao,*[a] Rong Zhang,[b] Yuezhen Bin,[b] and Jieshan Qiu*[a]**

***Received (in XXX, XXX) Xth XXXXXXXXX 20XX, Accepted Xth XXXXXXXXX 20XX***

**DOI: 10.1039/b000000x**

We reported a convenient and effective method to fabricate monolithic and conductive nanocomposites with various morphologies by directly infiltrating epoxy resin into pores of ultralight graphene aerogels (ULGAs) with desired m, followed by curing. The composites show linear ohmic behavior even with graphene filling content as low as 0.28 wt.%. The electrical conductivity of the composites can be modulated in the range from $3.3\times10^{-2}$ to $4.8\times10^{-1}$ $S.m^{-1}$, superior to that of traditional composites by directly mixing the powdery graphene with polymer. Furthermore, the conductivity of the nanocomposites remains unchanged in a wide range of temperature which may allow the structures as promising candidates as resistance elements for integrated circuits (ICs).

## 1 Introduction

Polymer-based composites, as a new paradigm for materials, have attracted tremendous attentions for their wide applications ranging from electrical and thermal management through structure media, to sensors and actuators mainly due to the synergistic effects arising from the interactions between different components.[1-6] By dispersing strong and conductive nanofillers,[7-9] such as graphene into the polymer matrices, lightweight composites can be fabricated with enhanced mechanical or electrical properties.[10-16] The optimized performances, especially conductivity, generally require the generation of continuous networks of graphene within polymer matrices at low filling content.[17,18] As such, uniform dispersion of fillers and the formation of strong contacts among them are urgently demanded. To address these challenges, a wealth of methods involving long time sonication and high shear mixing have been proposed to uniformly disperse graphene powder into polymer matrices which inevitably result in impaired properties of the fillers and tedious fabrication process.[19] The alternative gel-based patterning process[20] has partially circumvented these disadvantages but problems such as introduction of unexpected components into the final composites still need to be fixed. Thus, formation of continuous networks of graphene in polymer matrices at low loading remains a great challenge.

Graphene aerogels (GAs), a new form of three-dimensional (3D) continuous network, have attracted tremendous attentions recently due to their characteristics such as light weight, high porosity, large surface area and electrical conductivity.[21-29] Various methods have been proposed to assemble chemically converted graphene into monolithic structure.[21-25,27,28,30-34] However, most of the reported approaches encounter the problem of heavily restacking of graphene nanosheets and reduced porosity.[21,27,28] In this regard, we presented a strategy of functionalization-lyophilization-microwave treatment for the synthesis of electrically conductive and ultralight GAs (ULGAs) with extremely low density and ultra-high porosity.[22] The typical synthesis process involves the partial reduction and functionalization of graphene oxide with ethylenediamine (EDA) via which the surface of the nanosheets can be grafted with EDA. Thus, the restacking of graphene nanosheets during assembly can be hindered. Coupled with subsequent freeze-drying, the resulted structures show high porosity and large pores with size ranging from several tens to hundreds of micrometers. Then the freeze-dried aerogels are irradiated under microwaves to enhance the interaction among building blocks, giving rise to the final structure. The characteristics provided by ULGA may allow facile and efficient polymer infusion and composite fabrication. Based on this consideration, a polymer casting method has been proposed where ULGA acts as scaffold to achieve conductive polymer-based composite with extremely low graphene loading. This alternative strategy developed here has greatly simplified the process of fabrication of polymer-based composites by avoiding longtime sonication and high shear mixing. Furthermore, the conductivity of our composites is highly stable over a wide temperature range, making the corresponding structures promising candidates as resistance elements for integrated circuits (ICs).[35]

## 2 Experimental

### Synthesis of ULGAs

The ULGAs have been synthesized via a modified method reported previously.[22] In a typical preparing process, 5 mL of GO

dispersion with concentration of 3 mg.mL$^{-1}$ was loaded into a glass vial with inner diameter of 18 mm. Then, 20 μL of ethylenediamine (EDA) was added into the dispersion. After that, the mixture was heated at 95 °C for 6h. The freeze-dried sample was then irradiated under microwaves (800 W) for 1 min to give rise to ULGA. ULGA with various sizes and morphologies can be easily obtained by tuning the amount of reagents and the shape of reaction container. We also synthesized ULGA with much larger size where 75 mL of GO dispersion (3 mg.mL$^{-1}$) and 300 μL of EDA were involved for the production of single ULGA and the glass vial used here show inner diameter of 28 mm. The larger structure was then cut into different shape to fabricate ER/ULGA with different morphologies. The amount of GO and agents for the synthesis of ULGA with desired properties are listed in Table S1.

**Synthesis of thermal expanded graphene powder**

The thermal expanded graphene was synthesized according to a method reported elsewhere.[36] In a typical process, 0.2 g GO powder was loaded in a quartz tube and flushed with nitrogen thoroughly. Then, the tube was quickly inserted into a furnace preheated to 800 °C and rested for 2 minute to allow fully exfoliation and deoxygenation of GO. The powder was collected after cooling down to room temperature naturally.

**Fabrication of Epoxy Resin (ER)/ULGA**

The polymer involved in this research is ER (E44) and hexahydrophthalic anhydride serves as curing agent (Fig.S1). Typically, ER and curing agent with mass ratio of 100:85 were firstly blended at room temperature by agitation. The slurry was then heated at 60 °C for 2 h to make the mixture fluid. After that, the ULGAs were immersed into the mixture and then degassing at 60 °C under vaccum overnight. The fully impregenated ULGAs were taken out and curing. The curing process involves heating at 80 °C for 4h, heating at 140 °C for 4h and heating at 180 °C for 3h.

**Fabrication of ER-based composite with powdery fillers**

The mixture containing ER (E44) and curing agent (hexahydrophthalic anhydride) with mass ratio of 100:85 was heated at 60 °C for 2 h before adding the powdery graphene or CNTs. For the sake of dispersing the powders in the mixture uniformly, 30 minutes of sonication was applied. After degassing, a similar curing process was involved to produce this kind of ER-based composite.

**Characterization of composites**

The SEM observation was performed on a QUANTA 450 SEM. A slice of the composite was broken in liquid nitrogen to produce the fresh surface for observation. Raman spectra of ER, ULGA and ER/ULGA were performed on a DXR Raman Microscope (Thermo Scientific) with excitation wavelength of 532 nm. The *I-V* curves of the composite was recorded on an electrochemical workstation (CHI 760E) via a two-probe method. The conductivity of insulating sample was conducted on a HP 4339B high resistance meter.

## 3 Results and discussion

The fabrication process is schematically illustrated in Fig.1a. Firstly, the highly porous ULGA is immersed into the ER and the strong affinity of graphene with the ER[17,37] (Fig.S1) as well as the ultra-large pore sizes allows the full immersion of ULGA into the highly viscous fluid (Fig.1b). Even though other porous monolith such as carbon nanotube sponge has been selectively as scaffold to incorporate with ER, the polymer infiltration required the viscous fluid being diluted with solvents to facilitate this process due to the smaller pores.[38] On the other hand, the addition of solvent is totally avoided when infiltration of ER into ULGAs. The elimination of additional solvents, undoubtedly, can greatly simplify the fabrication process of composites. Then, the ULGA filled with ER was transferred under vacuum to remove the gas bubbles, permitting the completely filling the pores of aerogel. After curing, the corresponding composite can be obtained as shown in Fig.1c.

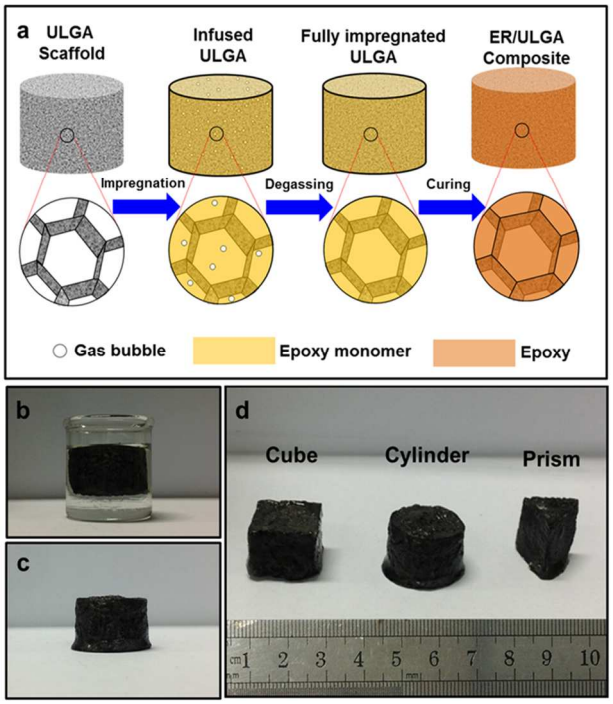


**Fig.1** (a) Schematic illustration of fabrication process of ER/ULGA, (b) digital image of ULGA impregnated into ER, (c) digital image of as-prepared ER/ULGA nanocomposite and (d) ER/ULGAs with different morphologies.

As shown in Fig.1b and c, the monolithic structure can survive polymer infiltration and manipulation in the highly viscous liquid, indicative of the strong interactions among building blocks. The GA scaffolds can be conveniently synthesized or processed into any shape.[28,39] Thus, the composites with various morphologies such as cube, cylinder and prism (Fig.1d) and different sizes (Fig.S2) can be easily synthesized by carrying out the fabrication process on ULGAs with desired morphologies or sizes. The microscopic observation of the composites is exhibited in Fig.2. As shown, the pores of ULGA (Fig.2a) are fully occupied by the ER (Fig.2b) while the graphene networks are well preserved. The observation of interface where graphene and polymer interact with each other reveals the absence of void indicating that graphene nanosheets are tightly adhered to the polymer. Furthermore, the graphene-based cellular walls exhibit wrinkled

topology and the roughness is highly demanded to improve the interlocking with polymer.[11] Fig.2d displays the Raman spectra of ER, ULGA and their composite. The pure ER shows a series of peaks associated with typical epoxies[40] (Table S2), while the ULGA displays peaks at 1350 and 1576 $cm^{-1}$ related to the D and G band of graphene. The spectrum of composite obtained by illuminating the interface exhibits all the peaks of ER and ULGA at the same position except the red shift of G band from 1576 $cm^{-1}$ for ULGA to 1585 $cm^{-1}$ for ER/ULGA. The shift of G band of carbon materials is highly related to the charge transfer between carbon and other components.[41] Thus, the shift of G band may indicate the formation of chemical bonds associated with possible ring-opening reactions and esterification reactions among ER, curing agent and functional groups such as hydroxyl groups on graphene (Fig.S3 and Fig.S4).[42]

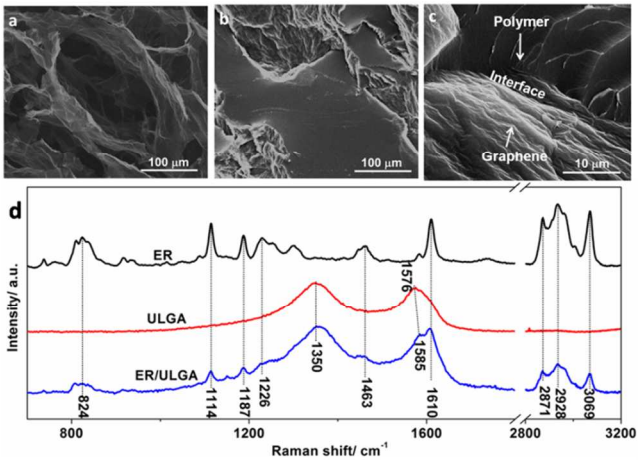


**Fig.2** SEM images of ULGA (a) and ER/ULGA at low (b) and high (c) magnification.(d) Raman spectra of ER, ULGA and ER/ULGA.

Originally, the ER is featured with insulation with electrical conductivity in the order of magnitude of $10^{-7}$ $S.m^{-1}$ while the ULGA is highly conductive shown in Fig.3a. After combining them together, the ER/ULGA gives a conductivity of $3.1\times10^{-1}$ $S.m^{-1}$ even with graphene content as low as 0.42 wt.% (Fig.3a), six orders of magnitude higher than that of ER, indicative of the well-maintained conductive network of graphene within the polymer matrix at low filling content. This result is in good agreement with the SEM observations (Fig.2 b and c). The slight decrease in conductivity from ULGA to ER/ULGA may associate with the formation of chemical bonds on the outmost graphene layers of the cellular walls. Commercially available CNT powder and thermal expanded graphene powder have also been introduced into the ER matrix with filling content of 0.42 wt.%. The corresponding compositions containing these powdery fillers defined as ER/CNT(p) and ER/G(p), however, still remain insulating, revealing the difficulty in formation of conductive networks with powdery fillers in the polymer matrices at low filling content. The SEM images (Fig. S5) of these composites reveal the inhomogeneous distribution and the absence of continuous networks of the fillers. A series of composites with other kinds of GAs as scaffolds have also been fabricated. The GAs involved here are synthesized by L-ascorbic acid-mediated reduction,[27] sodium bisulfite-mediated reduction[28] and hydrothermal-mediated reduction[21] of GO and the composites are named as ER/GA(L), ER/GA(S) and ER/GA(H) respectively. ER/ULGA shows a density equal to that of ER indicating the pores are totally filled with ER, whereas all the other composites exhibit the decreased density with void from 8% to 15% indicating the incompletely filled pores. The difference in filling effectiveness may derive from the different pore size distribution. The ULGAs mainly contain pores in the range of several tens to hundreds of μm (Fig.2a) where the transportation of highly viscous liquid such as ER is facilitated,[43] while other GAs with much smaller pores (Fig S6) show difficulty in permitting the transportation of viscous liquids within pores.

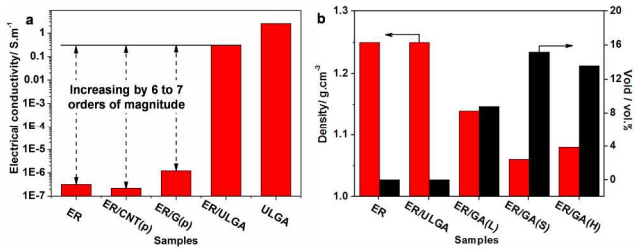


**Fig.3** (a) Comparison of conductivity of nanocomposites with CNT powder, graphene powder and ULGA as fillers. (b) Comparison of density and void of nanocomposites with different GAs as fillers.

A serial of ER/ULGA composites have been fabricated by infiltrating ER into ULGA scaffolds with different density. Fig.4a shows the *I-V* curves of different ER/ULGAs where all the curves exhibit linear ohmic behavior indicating the continuous networks are well-maintained in all these samples. The adoption of ULGAs with different density as scaffold can give rise to the final *I-V* curves with different slopes suggesting an effective way to modulate the conductivity of the composites. The filling fraction was calculated and the weight percentage of graphene can be changed from 0.28 to 0.47 wt.% making the filling content of graphene among the lowest level.[17,20] Nevertheless, the bulk conductivity of the corresponding composites ranges from $3.3\times10^{-2}$ to $4.8\times10^{-1}$ $S.m^{-1}$, superior to that of graphene filled polymer structures produced via traditional methods (Fig.S7).[17] This observation further confirms the efficiency of our suggestion for the production of high performance polymer-based composite.

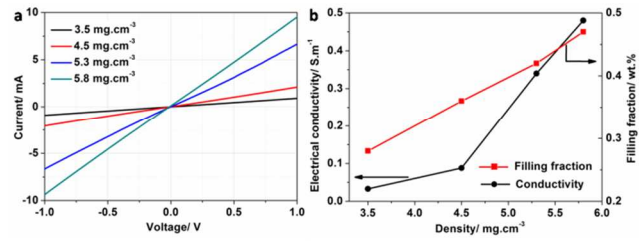


**Fig.4** (a) *I-V* curves and (b) comparison of conductivity and filling fraction of nanocomposites with ULGAs of different density.

The *I-V* curves of the composite in the temperature range from 25 to 100 °C were tested on a setup illustrated in Fig.5a. After being glued between two plates by silver paste with two metal wires connected to electrochemical workstation, the composite has been placed on a heating plate allowing the temperature of the composite to rise accordingly. The corresponding *I-V* curves are exhibited in Fig.S8 and inset of Fig.5b. As shown, all these curves give a linear behavior, indicating ohmic contact over this

temperature. Furthermore, the bulk conductivities of ER/ULGA at different temperature are compared in Fig.5b. For clarity, the conductivities tested at different temperature have been divided by the conductivity at 25 °C. The structure gives a stable electrical performance with almost unchanged bulk resistance over this temperature range. The temperature-resistance property of polymer composite depends on several factors including conductive mechanisms,[44] properties of fillers[45] and the thermal expansion performance of different components. The continuous network formed by the interaction among these nanosheets, the delimited region for the movement of electrons provided by the graphene (Fig.S9) and so on make the bulk resistance of ER/ULGA almost temperature-independent. As it's known to all, the performances of electronic devices are highly temperature-denpendent.[35,46,47] The extra heat generated during running high power integrated circuits (ICs) can be removed by cooling to keep the temperature from exceeding 100 °C.[35,46,47] However, the properties such as resistivity of many materials still change greatly even from room temperature to 100 °C [48] which will impair the performance of ICs. Thus, the development of materials with stable electrical conductivity over this temperature range is urgently demanded. The electrical performance provided by our composite may allow the ICs to run smoothly at a wide temperature range.

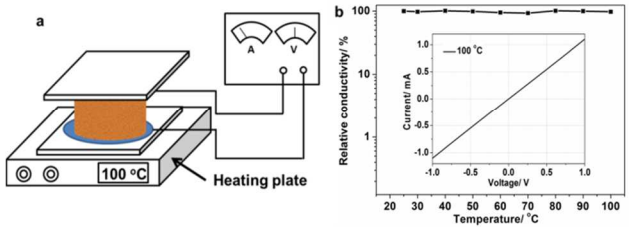


**Fig.5** (a) Illustration of test setup of conductivity of nanocomposite at elevated temperature. (b) The conductivity of nanocompostie as a function of temperature and inset shows the I-V curve tested at 100 °C

## 4 Conclusions

In summary, we have demonstrated an efficient approach to monolithic and conductive nanocomposites with various morphologies by directly infiltrating ER into pores of ULGAs with desired shapes, followed by curing. The ultra-large pores of ULGAs facilitate the completely filling the pores with polymer, while the extremely low density allows ultralow loading content to achieve conductivity. The filling fraction of graphene can be modulated in the range from 0.28 to 0.47 wt.% by infiltrating ER into ULGAs with different density. Accordingly, the electrical conductivity varies from $3.3\times10^{-2}$ to $4.8\times10^{-1}$ S.m$^{-1}$, superior to the composites by directly mixing powdery graphene with polymer. Furthermore, the conductivity of the composite is temperature-independent at least in the temperature range from 25 to 100 °C. This superior conductivity-temperature property may allow the composites promising candidates as resistance elements for ICs. The method developed here may inspire new possibilities for the production of high performance polymer-based composite in cost- and energy- efficient manners.

## Acknowledgements

This work was supported by the NSFC (grants 51072028, 20836002).

## Notes and references

[a] *Carbon Research Laboratory, Liaoning Key Lab for Energy Materials and Chemical Engineering, State Key Lab of Fine Chemicals, School of Chemical Engineering, Dalian University of Technology, Dalian 116024, China; E-mail: zbzhao@dlut.edu.cn, jqiu@dlut.edu.cn*
[b] *Department of Polymer Material Science, Dalian University of Technology, Dalian 116024, China.*
† Electronic Supplementary Information (ESI) available: See DOI: 10.1039/b000000x/

1 H. Bai, C. Li and G. Q. Shi, *Adv. Mater.* , 2011, **23**, 1089.
2 Z. Spitalsky, D. Tasis, K. Papagelis and C. Galiotis, *Prog. Polym. Sci.* , 2010, **35**, 357.
3 Z. H. Yang, Z. Cao, H. Sun and Y. Li, *Adv. Mater.*, 2008, **20**, 2201.
4 S. Isaji, Y. Z. Bin and M. Matsuo, *Polymer*, 2009, **50**, 1046.
5 V. N. Mochalin, I. Neitzel, B. J. M. Etzold, A. Peterson, G. Palmese and Y. Gogotsi, *ACS Nano*, 2011, **5**, 7494.
6 I. Neitzel, V. N. Mochalin, J. Niu, J. Cuadra, A. Kontsos, G. R. Palmese and Y. Gogotsi, *Polymer*, 2012, **53**, 5965.
7 M. Q. Zhao, Q. Zhang, X. L. Jia, J. Q. Huang, Y. H. Zhang and F. Wei, *Adv. Funct. Mater.* , 2010, **20**, 677.
8 P. M. Ajayan, L. S. Schadler, C. Giannaris and A. Rubio, *Adv. Mater.* , 2000, **12**, 750.
9 K. H. Kim, M. Vural and M. F. Islam, *Adv. Mater.* , 2011, **23**, 2865.
10 S. Stankovich, D. A. Dikin, G. H. B. Dommett, K. M. Kohlhaas, E. J. Zimney, E. A. Stach, R. D. Piner, S. T. Nguyen and R. S. Ruoff, *Nature*, 2006, **442**, 282.
11 T. Ramanathan, A. A. Abdala, S. Stankovich, D. A. Dikin, M. Herrera-Alonso, R. D. Piner, D. H. Adamson, H. C. Schniepp, X. Chen, R. S. Ruoff, S. T. Nguyen, I. A. Aksay, R. K. Prud'homme and L. C. Brinson, *Nat. Nanotechnol.* , 2008, **3**, 327.
12 H. F. Yang, C. S. Shan, F. H. Li, Q. X. Zhang, D. X. Han and L. Niu, *J. Mater. Chem.* , 2009, **19**, 8856.
13 K. S. Kim, I. Y. Jeon, S. N. Ahn, Y. D. Kwon and J. B. Baek, *J. Mater. Chem.* , 2011, **21**, 7337.
14 V. H. Luan, H. N. Tien, T. V. Cuong, B. S. Kong, J. S. Chung, E. J. Kim and S. H. Hur, *J. Mater. Chem.* , 2012, **22**, 8649.
15 T. Wei, G. L. Luo, Z. J. Fan, C. Zheng, J. Yan, C. Z. Yao, W. F. Li and C. Zhang, *Carbon*, 2009, **47**, 2296.
16 X. Z. Hu, Z. Xu and C. Gao, *Sci.Rep.*, 2012, **2**,767.
17 J. H. Du and H. M. Cheng, *Macromol. Chem. Phys.*, 2012, **213**, 1060.
18 X. Y. Qi, D. Yan, Z. G. Jiang, Y. K. Cao, Z. Z. Yu, F. Yavari and N. Koratkar, *ACS Appl. Mat. Interfaces* 2011, **3**, 3130.
19 J. J. Liang, Y. Wang, Y. Huang, Y. F. Ma, Z. F. Liu, F. M. Cai, C. D. Zhang, H. J. Gao and Y. S. Chen, *Carbon*, 2009, **47**, 922.
20 F. Irin, S. Das, F. O. Atore and M. J. Green, *Langmuir*, 2013, **29**, 11449.
21 Y. X. Xu, K. X. Sheng, C. Li and G. Q. Shi, *ACS Nano*, 2010, **4**, 4324.
22 H. Hu, Z. Zhao, W. Wan, Y. Gogotsi and J. Qiu, *Adv. Mater.* , 2013, **25**, 2219.
23 Z. Q. Niu, J. Chen, H. H. Hng, J. Ma and X. D. Chen, *Adv. Mater.* , 2012, **24**, 4144.
24 H. Y. Sun, Z. Xu and C. Gao, *Adv. Mater.* , 2013, **25**, 2554.
25 Y. Zhao, J. Liu, Y. Hu, H. H. Cheng, C. G. Hu, C. C. Jiang, L. Jiang, A. Y. Cao and L. T. Qu, *Adv. Mater.* , 2013, **25**, 591.
26 Z. H. Tang, S. L. Shen, J. Zhuang and X. Wang, *Angew. Chem. Int. Ed.* , 2010, **49**, 4603.
27 X. T. Zhang, Z. Y. Sui, B. Xu, S. F. Yue, Y. J. Luo, W. C. Zhan and B. Liu, *J. Mater. Chem.* , 2011, **21**, 6494.
28 L. F. Yan and W. F. Chen, *Nanoscale*, 2011, **3**, 3132.
29 Z. P. Chen, W. C. Ren, L. B. Gao, B. L. Liu, S. F. Pei and H. M. Cheng, *Nat. Mater.* , 2011, **10**, 424
30 H.-P. Cong, X.-C. Ren, P. Wang and S.-H. Yu, *ACS Nano*, 2012, **6**, 2693.

31 H. Huang, P. W. Chen, X. T. Zhang, Y. Lu and W. C. Zhan, *Small*, 2013, **9**, 1397.
32 L. Chen, B. Wei, X. T. Zhang and C. Li, *Small*, 2013, **9**, 2331.
33 Z. Y. Sui, Q. H. Meng, X. T. Zhang, R. Ma and B. Cao, *J. Mater. Chem.* , 2012, **22**, 8767.
34 L. Chen, X. J. Wang, X. T. Zhang and H. M. Zhang, *J. Mater. Chem.* , 2012, **22**, 22090.
35 R. Prasher, *Science*, 2010, **328**, 185
36 M. J. McAllister, J. L. Li, D. H. Adamson, H. C. Schniepp, A. A. Abdala, J. Liu, M. Herrera-Alonso, D. L. Milius, R. Car, R. K. Prud'homme and I. A. Aksay, *Chem. Mater.* , 2007, **19**, 4396.
37 R. Verdejo, M. M. Bernal, L. J. Romasanta and M. A. Lopez-Manchado, *J. Mater. Chem.* , 2011, **21**, 3301.
38 X. C. Gui, H. B. Li, L. H. Zhang, Y. Jia, L. Liu, Z. Li, J. Q. Wei, K. L. Wang, H. W. Zhu, Z. K. Tang, D. H. Wu and A. Y. Cao, *ACS Nano*, 2011, **5**, 4276.
39 H. Bi, K. Yin, X. Xie, Y. Zhou, N. Wan, F. Xu, F. Banhart, L. Sun and R. S. Ruoff, *Adv. Mater.* , 2012, **24**, 5124.
40 S. Farquharson, W. Smith, E. Rigas, D.Granville, *Proc. SPIE*, 2001, **103**,103.
41 G. M. Zhou, D. W. Wang, L. C. Yin, N. Li, F. Li and H. M. Cheng, *ACS Nano*, 2012, **6**, 3214.
42 W.Potter. *Epoxide Resins*. London: Iliffle Books; 1970.
43 Y. Nishi, N. Iwashita, Y. Sawada and M. Inagaki, *Water Res.* , 2002, **36**, 5029.
44 Scarisbr.Rm, *J. Phys. D-Appl. Phys.*, 1973, **6**, 2098.
45 K. G. Princy, R. Joseph and C. S. Kartha, *J. Appl. Polym. Sci.* , 1998, **69**, 1043.
46 A. Majumdar, *Nat. Nanotechnol.* , 2009, **4**, 214.
47 I. Chowdhury, R. Prasher, K. Lofgreen, G. Chrysler, S. Narasimhan, R. Mahajan, D. Koester, R. Alley and R. Venkatasubramanian, *Nat. Nanotechnol.* , 2009, **4**, 235
48 L. G. Gai, G. J. Du, Z. Y. Zuo, Y. M. Wang, D. Liu and H. Liu, J. Phys. Chem. C 2009, 113, 7610